DOI: 10.18721/JPM.14105
UDC 532.542.4

A FLOW IN THE BLOOD VESSEL WITH A ONE-SIDE STENOSIS: NUMERICAL STUDY OF THE STRUCTURE AND LOCAL TURBULIZATION

Ya.A. Gataulin, E.M. Smirnov

Peter the Great St. Petersburg Polytechnic University,
St. Petersburg, Russian Federation

In the paper, the LES results of a flow by using a model of the blood vessel with a one-side 70% stenosis, at a Reynolds number of 1803, have been presented. The Germano – Lilly model was applied to subgrid viscosity evaluation. A jet-like zone and a recirculation one were found to stand out just behind the stenosis, and a pair of secondary-flow vortices forms being within each of them. Instabilities of the mixing layer initiated the flow turbulence with formation of vortex structures of different scales at the boundary between the reverse flow zone and the jet. These structures filled the whole cross-section of the vessel about the flow attachment point. Turbulent shear stresses were significant in magnitude only at a flow section of about four-caliber length. Further downstream, the flow relaminarised.

Keywords: blood flow, stenosis, turbulence, numerical simulation, large eddy simulation

Citation: Gataulin Ya.A., Smirnov E.M., A flow in the blood vessel with a one-side stenosis: numerical study of the structure and local turbulization, St. Petersburg Polytechnical State University Journal. Physics and Mathematics. 14 (1) (2021) 69–80. DOI: 10.18721/JPM.14105

This is an open access article under the CC BY-NC 4.0 license (https://creativecommons.org/licenses/by-nc/4.0/)

ЧИСЛЕННОЕ ИССЛЕДОВАНИЕ СТРУКТУРЫ И ЛОКАЛЬНОЙ ТУРБУЛИЗАЦИИ ТЕЧЕНИЯ В КРОВЕНОСНОМ СОСУДЕ С ОДНОСТОРОННИМ СТЕНОЗОМ

Я.А. Гатаулин, Е.М. Смирнов

Санкт-Петербургский политехнический университет Петра Великого,
Санкт-Петербург, Российская Федерация

В статье представлены результаты расчетов течения в модели кровеносного сосуда с односторонним стенозом 70 % при числе Рейнольдса, равном 1803. Численное решение получено методом моделирования крупных вихрей по динамической модели Джермано – Лилли для оценки подсеточной вязкости. Установлено, что непосредственно за стенозом в потоке выделяются 2 зоны: струйного течения и обширная рециркуляционная, а в каждой присутствует пара вихрей вторичного течения. Неустойчивости слоя смешения на границе струи и зоны обратного течения инициируют турбулизацию потока с образованием разномасштабных вихревых структур. Последние заполняют все поперечное сечение сосуда в окрестности точки присоединения. Турбулентные напряжения значительны по величине лишь на участке длиной около четырех калибров. Вниз по потоку течение реламинаризируется.

Ключевые слова: кровоток, стеноз, турбулентность, численное моделирование, метод моделирования крупных вихрей

Ссылка при цитировании: Гатаулин Я.А., Смирнов Е.М. Численное исследование структуры и локальной турбулизации течения в кровеносном сосуде с односторонним стенозом // Научно-технические ведомости СПбГПУ. Физико-математические науки. 2021. Т. 14. № 1. С. 69–80. DOI: 10.18721/JPM.14105

Статья открытого доступа, распространяемая по лицензии CC BY-NC 4.0 (https://creativecommons.org/licenses/by-nc/4.0/)

Introduction

Modern computational fluid dynamics (CFD) offers the broadest range of tools for simulating blood flow in various segments of the vascular bed. Laminar flow is established in small and medium-sized vessels, where the Reynolds number Re does not exceed 1000. We considered the spatial structure of laminar flow in carotid artery models, including the case of stenotic vessels (persistent narrowing of its lumen), in several earlier studies [1 – 3]. However, the flow behind the stenosis in large blood vessels is characterized by higher values of the Reynolds number and is particularly difficult to compute. The flow behind the stenosis in such vessels actually turns out to be cyclically transient, since it is locally turbulent during a period in the cardiac cycle, remaining completely laminar for the rest of the cycle. Developing approaches to simulation of the turbulence occurring locally holds the key to obtaining sufficiently reliable predictions.

Turbulent flows in stenotic vessels are traditionally computed using models based on the Reynolds-Averaged Navier – Stokes equations (RANS) [4 – 7]. It was established that RANS models are capable of providing good agreement between the computed field of averaged velocity and the measured data; however, the predictions obtained for some turbulence characteristics that are interesting for biomedical applications turn out to have very low quality.

Direct Numerical Simulation (DNS) [8 – 11] and eddy-resolving models (including primarily Large Eddy Simulation or LES) [12 – 15] have become widely popular in recent years for improving the quality of numerical analysis of turbulent flows in stenotic vessels. All components of unsteady vortex motion are completely resolved within the DNS method, which means that the computational costs for obtaining a numerical solution are high, rapidly increasing with an increase in the Reynolds number. The much less expensive LES method only numerically reproduces sufficiently large eddies, which are characterized by energy transfer, while eddies of a smaller scale are simulated using subgrid-scale models (SGS).

Most of the applied computations by the LES method are carried out using the classical Smagorinsky model introducing subgrid-scale turbulent viscosity. This model was developed assuming a sufficiently developed turbulence, which for practical applications is reduced to the condition that the subgrid-scale viscosities be considerably higher than the molecular ones. The Smagorinsky model with a constant empirical coefficient C_S in the formula for calculating the subgrid-scale viscosity is ill-suited for flows with a transient nature of motion (from laminar to turbulent).

Germano et al. [16] expanded the capabilities of the Smagorinsky algebraic model, in particular for the case of transient flows, developing the so-called dynamic model, where the coefficient CS is not given but calculated based on the expression obtained by applying a double filtering procedure to the velocity field. Lilly [17] later proposed a modification of the dynamic model, important for practical applications, which consists in cutting off the locally negative values of the coefficient C_S at zero. The Germano-Lilly dynamic model was successfully applied in [14] for LES computations of transient regimes in statistically two-dimensional pulsatile flow in a channel with local one-sided narrowing (stenosis model) by 50%; the peak values of the Reynolds number reached 2000; the periodic boundary conditions were imposed in the third direction.

This paper presents numerical analysis for transient three-dimensional flow of an incompressible viscous fluid in a blood vessel model with unilateral stenosis of 70% at a constant flow rate corresponding to the Reynolds number Re = 1803.

The geometry of the stenosis is identical to one of the cases described in the recent experimental work [18], using digital tracer imaging (Particle Image Velocimetry, PIV) to measure the characteristics of pulsatile flow (with a peak value of

Re = 1803). Simulations using the CFD software package ANSYS CFX 18.2 were performed based on the large eddy simulation method with the Germano – Lilly dynamic model for computing the subgrid-scale viscosity.

Problem statement and computational aspects

The geometric model of the vessel with unilateral stenosis (Fig. 1) is borrowed from the experimental study [18]. The vessel beyond the boundaries of the stenosis is a tube with the diameter D. Let us introduce the Cartesian coordinate system x, y, z, whose origin is located in the section with the narrowest lumen; the z axis is directed along the vessel, and the y axis is directed towards the non-stenotic (provisionally upper) wall. The geometry of the stenosis that is symmetrical about the central longitudinal plane $x = 0$ is described by the following formulas:

$$\frac{d(z)}{D} = \left(1 - \frac{S}{200}\right) - \frac{S}{200}\cos\left(\frac{2z\pi}{L}\right), \quad -\frac{L}{2} \le z \le \frac{L}{2};$$

$$\frac{c(z)}{D} = 1 - \frac{d(z)}{2D}, \quad -\frac{L}{2} \le z \le \frac{L}{2},$$

where d is the local lumen diameter in the stenotic region, L is the length of the stenosis, s is the coordinate of the lumen center along the axis y (counted from the lower wall, as adopted here and below),

$$S = (1 - d_{min}/D)\cdot 100\ \%$$

(d_{min} is the minimum local diameter d).

In the case considered, $S = 45\%$, $L = 2D$, while the area of the narrowest section in the stenotic region is 30.25% of the cross-sectional area of the tube beyond the stenosis, i.e., the stenosis amounts to 69.75% (70% rounded off).

The flow in this model of a blood vessel at Re = 1803 was computed by the LES method using the Germano – Lilly dynamic model [16, 17]. The computational domain included a stenotic region, an inlet section with the length of $5D$ and an outlet section with the length of $20D$; the latter is sufficient for eliminating any significant influence of the outlet boundary condition on the flow near the stenosis.

The computations were carried out using the general-purpose 'finite-volume' CFD code ANSYS CFX, version 18.2. This software tool operates with dimensional values.

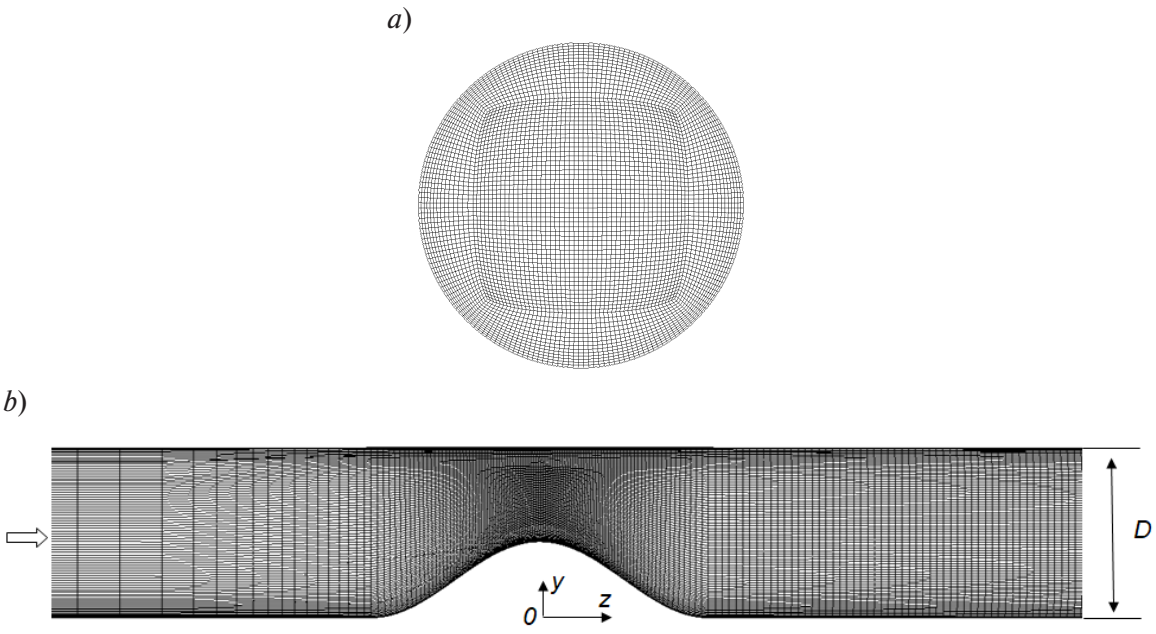

Fig. 1. View of computational mesh in transverse (*a*) and longitudinal (*b*) sections of the vessel with stenosis

Table

Computational parameters and their values

Parameter	Notation	Unit of measurement	Value
Vessel diameter (beyond stenosis)	D	mm	10
Mean flow velocity (beyond stenosis)	V_b	m/s	0.627
Fluid density	ρ	kg/m^3	1000
Dynamic viscosity coefficient	μ	Pa·s	0.003478
Reynolds number	$\mathrm{Re} = \rho V_b D/\mu$		1803

The set of defining dimensional parameters of the problem is given in the table. The Reynolds number is computed from these parameters.

A parabolic velocity distribution was given at the inlet to the computational domain, which corresponds to the Poiseuille solution for developed laminar flow in a circular tube; constant pressure and 'soft' conditions for the velocity were imposed at the outlet. No-slip conditions were imposed on the walls.

The ICEM CFD program was used to construct a computational *O-grid* mesh consisting of hexahedral elements (Fig. 1). The longitudinal mesh spacing was uniform in the stenotic region and throughout the entire outlet section, amounting to $0.04D$, while the maximum transverse spacing was $0.02D$. The longitudinal spacing at the inlet section gradually decreased to $0.04D$ approaching the stenotic region. The total number of elements in the mesh was about 4.5 million.

A central scheme with second-order accuracy was used in the computations for approximating the convective terms in the equations of motion. A three-layer Euler scheme was used to advance in time. The time step was 0.0002 s, which ensured local Courant numbers less than unity in the entire computational domain.

The sample used to obtain the averaged flow characteristics was accumulated over a time of $1050t_s$, where t_s is the time scale of the problem ($t_s = D/V_b$); the previous time interval, covering about $600t_s$, was sufficient for statistically steady flow to be established, starting from a zero velocity field.

The simulations were performed on the Politechnic RSC Tornado cluster of the Polytechnic Supercomputer Center (http://www.scc.spbstu.ru). The problem was run on 18 dual-core nodes (Intel (R) Xeon (R) E5 2697v3) and parallelized to 450 cores; the full simulation took about a week of real time (76,000 core hours).

Results and discussion

A peculiarity of the simulated flow is the presence of a laminar-turbulent transition behind the stenosis. To illustrate this, the Q-criterion isosurface was constructed in Fig. 2,*a* [19], with the colors corresponding to the local values of the velocity modulus; this allows visualizing the region where turbulent vortical structures with different scales evolve due to hydrodynamic instabilities. The latter are characteristic for jet-like shear flow.

Fig. 2 also shows two isosurfaces of the time-averaged longitudinal velocity component. One of these surfaces (see Fig. 2,*b*), plotted for the value $V_z = 3.2V_b = 2$ m/s, illustrates the dimensions of the region with pronounced jet flow. The other one (Fig. 2,*c*), corresponding to the value $V_z = -0.002V_b$, shows two zones of recirculation flow behind the stenosis: an extensive one (about $5D$-long) immediately behind the stenosis, and a very small one, located near the opposite wall at a distance of about $4D$ from the center of the stenosis. A small separation zone is also formed before the stenosis.

The fields of time-averaged velocity components in three cross sections of the vessel model are shown in Fig. 3. Evidently, the jet formed in the stenotic region, whose local velocities are relatively high (exceeding the mean flow rate $V_b = 0.627$ m/s beyond the stenosis by up to 4

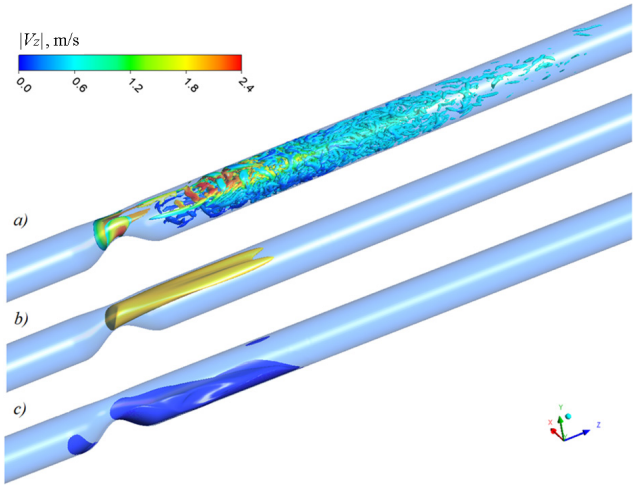

Fig. 2. Flow structures in stenotic vessel, visualized by constructing a Q-criterion isosurface ($Q = 0{,}06$ s^{-2}) (*a*); two isosurfaces of averaged longitudinal velocity V_z taking the values $3{,}2V_b$ (*b*) and $-0{,}002V_b$ (*c*)

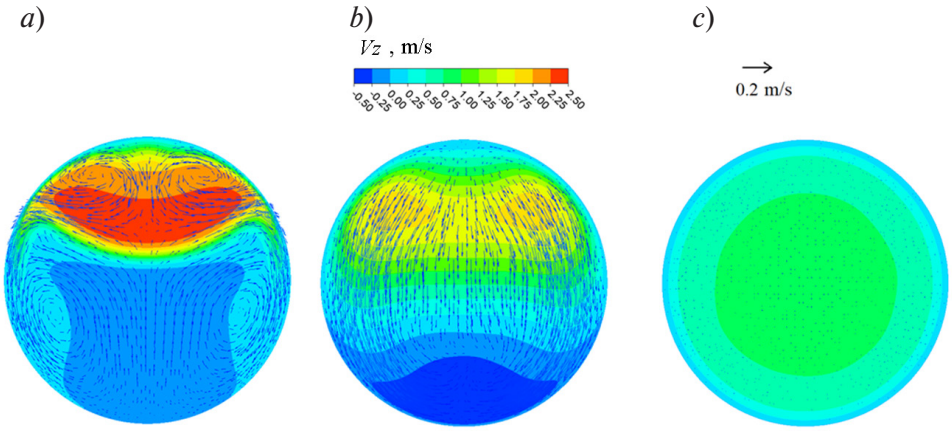

Fig. 3. The time-averaged field of longitudinal velocity component with the field of transverse velocity vectors superimposed on it in three sections of the vessel model: $z/D = 2$ (*a*), 4 (*b*), 10 (*c*)

times), is also characterized by the presence of a fairly intense transverse (secondary) flow in the form of a vortex pair (see Fig. 3,*a*). In fact, this pair, similar to Dean vortices in curved tubes, develops in the anterior part of the stenosis, where the flow occurs along curved streamlines following the geometry of the stenosis. In turn, the vortex pair developing in the stenosis induces a secondary flow (with opposite circulation) in the backflow zone behind the stenosis, also leading to bifurcation of the jet downstream (see Fig. 2,*b* and 3,*b*). The averaged transverse flow almost completely degenerates at a distance less than $10D$ from the center of the stenosis, and the distribution of the averaged longitudinal velocity regains an axisymmetric 'tubular' shape, with the maximum velocity in the center of the vessel (see Fig. 3,*c*).

The field of averaged longitudinal velocity in the central longitudinal section (in the plane of symmetry) is shown in Fig. 4,*a*. It can be seen here and in Fig. 3,*b* that the maximum velocity of the backflow section in the main recirculation zone is comparable in magnitude with the mean flow rate V_b beyond the stenosis.

A high-gradient shear layer (mixing layer) is formed at the boundary of the jet and the recirculation zone; the phenomena characteristic for this

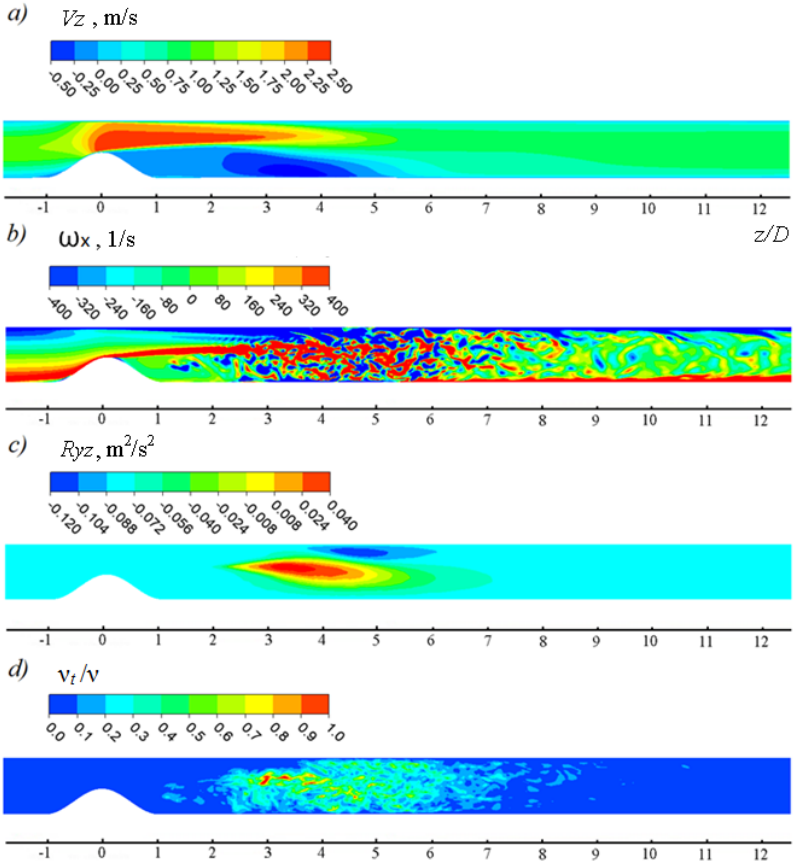

Fig. 4. Computed fields in the symmetry plane of the vessel: time-averaged longitudinal velocity (*a*), instantaneous value of *x*-component of vorticity (*b*), Reynolds shear stress $R_{yz} = R_{yz} = -\overline{V_y' V_z'}$ (*s*), instantaneous value of the ratio of subgrid-scale vortex to molecular viscosity (*d*)

layer are caused by the Kelvin – Helmholtz instability. Visualization for the instantaneous field of the x-component of the vorticity vector (Fig. 4,*b*) indicates that the Kelvin – Helmholtz instability and other hydrodynamic instabilities appearing in the presence of backflow and secondary flows generate turbulent flow with three-dimensional vortical structures of different scales evolving. These structures fill the entire cross section of the vessel in the neighborhood of the attachment point. However, the flow becomes relaminarized further downstream. It can be seen from Figs. 2,*a* and 4,*b* that as the distance from the stenosis increases, small-scale structures quickly disappear from the spectrum of pulsatile flow, while the remaining vortical structures with lower intensity stretch along the flow.

Fig. 4,*c* shows the field of values for one of the components of the Reynolds stress tensor computed from the numerically resolved components of pulsatile motion (marked with a prime; the overbar corresponds to averaging over time). It can be seen that the turbulent shear stress $R_{yz} = R_{yz} = -\overline{V_y' V_z'}$, playing a predominant role in extracting kinetic energy from the main flow, is significant in magnitude only at several calibers in the neighborhood of the attachment point, namely, at $2.5 < z/D < 6.5$. This is in agreement with the measurement data given in [18] for the generation rate of turbulent kinetic energy at the moment of the highest flow rate.

Determining the level of subgrid-scale kinematic viscosity predicted in our computations by the Germano – Lilly dynamic model gives the instantaneous field of the ratio of the subgrid-scale

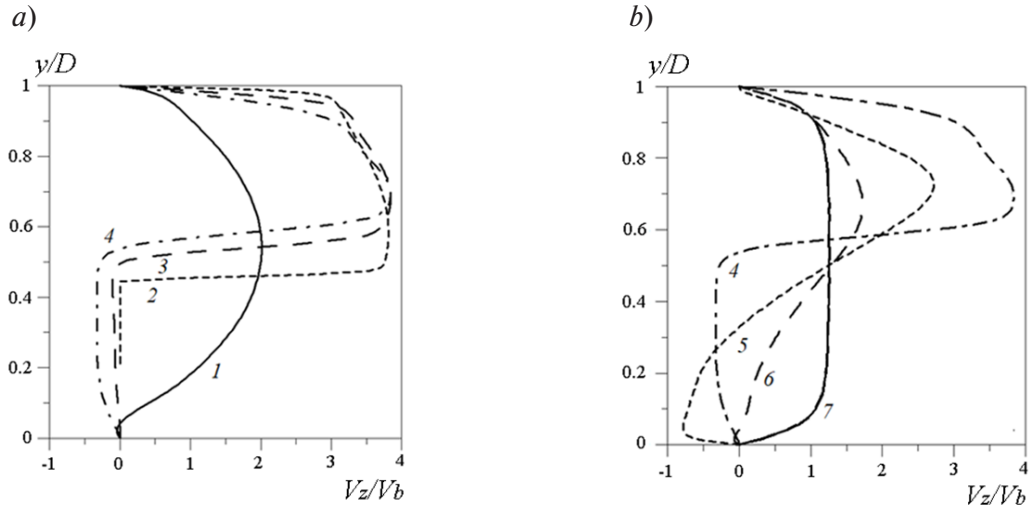

Fig. 5. Profiles of time-averaged longitudinal velocity in the symmetry plane, in different sections of the stenotic vessel; *a*): $z/D = -1$ (*1*), 0 (*2*), 1 (*3*), 2 (*4*); *b*): $z/D = 2$ (*4*), 4 (*5*), 5 (*6*), 10 (*7*)

vortex to molecular viscosity, shown in Fig. 4,*d*. We can conclude from these data that the contribution of subgrid-scale viscosity to dissipative effects in the given flow configuration, with Re = = 1803, is again significant only in the region covering several calibers in the neighborhood of the attachment point; moreover, even the ratio ν_t/ν is less than unity even in this region.

Fig. 5 shows the profiles of the time-averaged longitudinal component of velocity in the symmetry plane, normalized to the value of the mean flow velocity V_b for several cross sections of the flow in the stenotic region (two graphs are given for clarity). As the flow in the first half of the stenotic region is strongly accelerated, a flow core that is nearly homogeneous evolves in the center of the stenosis, with relatively thin high-gradient shear layers forming at the boundaries of the core (see Fig. 5,*a*). The upper part of the flow core is already largely smeared two calibers away from the center of the stenosis ($z/D = 2$); this is mainly due to convective transfer of low-velocity fluid from the wall, responsible for the above-mentioned secondary flow in the form of a vortex pair (see Fig. 3,*a*). At the same time, the high-gradient layer at the lower boundary is very pronounced up to this section. The nature of the velocity profiles is drastically different in the sections $z/D = 4$ and 5, located further downstream (Fig. 6,*b*): their central part is characterized by very moderate velocity gradients (see Fig. 5,*b*). The velocity profile related to the section $z/D = 10$ is a good illustration for the consequences of the mixing action of turbulent structures 'residing' in the neighborhood of the attachment point and some distance away from it: an almost axisymmetric central flow region develops as a result of this mixing (see also Fig. 3,*c*), with velocities close to mean flow rate, along with a boundary layer (gradually increasing in thickness with distance from the given section).

Longitudinal distributions of the time-averaged skin friction coefficient on the lower and upper walls of the vessel (in the symmetry plane) are shown in Fig. 6. The skin friction coefficient was calculated by the formula

$$C_f = \tau_w \Big/ \left(\rho V_b^2/2\right),$$

where τ_w is the modulus of the skin shear stress vector on the wall.

To identify the backflow zones, the values of the skin friction coefficient shown in the graphs were computed taking into account the sign of the longitudinal component τ_{wz} of the surface stress vector.

The skin friction coefficient is very high, exceeding the value of 0.00887 obtained for the flow before this region by almost 50 times. The

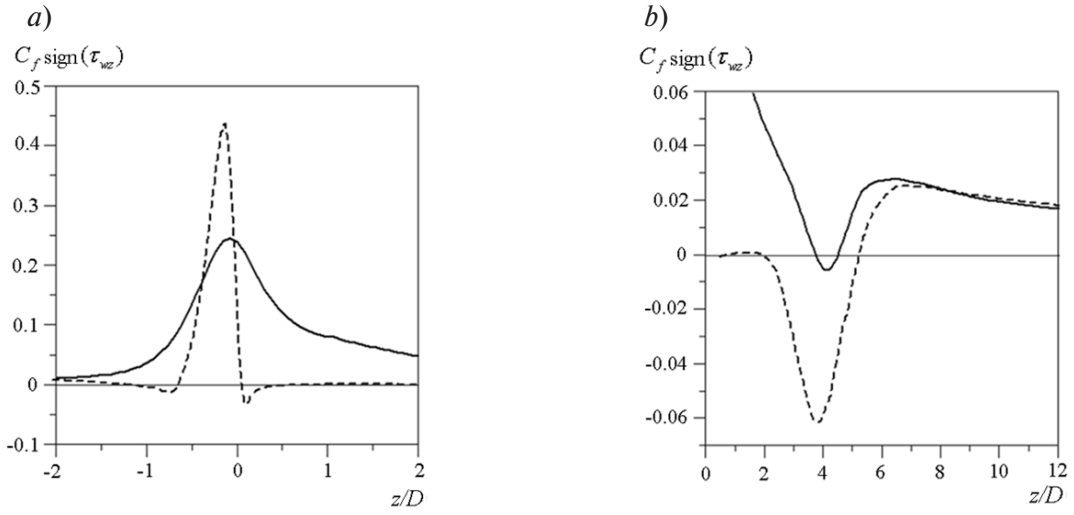

Fig. 6. Longitudinal changes in the time-averaged skin friction coefficient in the stenotic region (*a*) and behind it (*b*);
data are given for the upper (solid line) and lower (dashes) walls

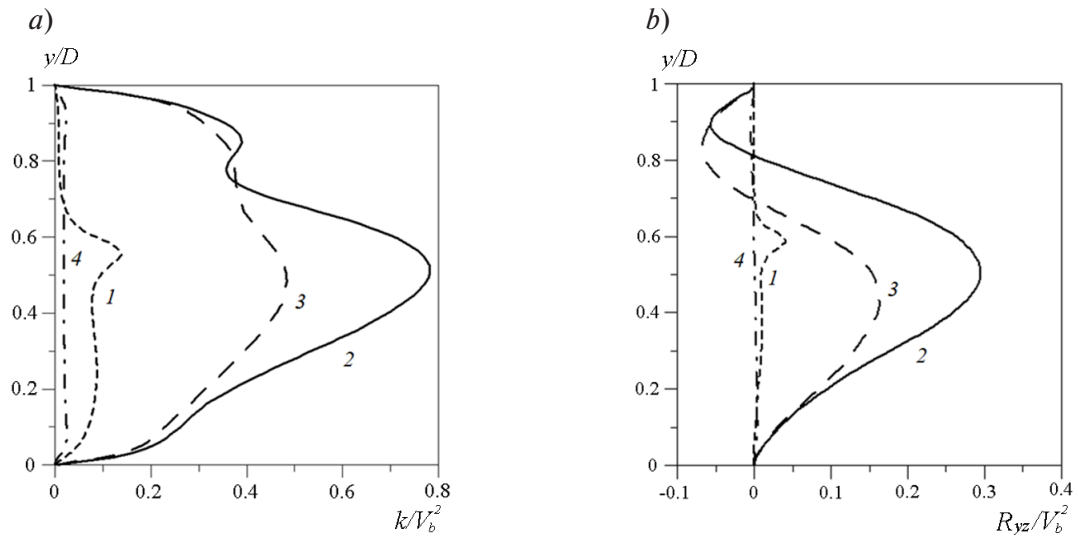

Fig. 7. Normalized profiles of turbulent kinetic energy of turbulence k (*a*) and Reynolds stress R_{yz} (*b*) in symmetry plane of the vessel for 4 sections located in the region behind the stenosis:
$z/D = 2$ (*1*), 4 (*2*), 5 (*3*), 10 (*4*)

values of C_f with the largest magnitude in the backflow zone are 7 times higher than those before the stenotic region. According to the computations performed, the attachment point of the flow in the symmetry plane is located at a distance $L_r = 5.3D$ from the center of the stenosis. This value is fairly close to the experimental estimate $L_r \cong 4.5D$, which follows from the data given in [18]. These data were obtained for the position of the attachment point during pulsatile flow, with the Reynolds numbers lying in the range 1000 – 1800.

Fig. 7 shows the profiles of two turbulence characteristics for four sections located behind the stenosis: turbulent kinetic energy k and the Reynolds stress R_{yz}; both are computed (for the symmetry plane) from the numerically resolved components of pulsatile motion and are normalized to the square of the mean flow rate. Notably, the turbulent kinetic energy in the sections

$z/D = 4$ and 5 is close in order of magnitude to the specific kinetic energy of the flow entering the stenotic region. The positions of the peak values of Reynolds stress and turbulent kinetic energy practically coincide for each of these cross sections, while the ratios $R_{yz,peak}/k_{peak}$ are approximately 0.38 and 0.35 for the cross sections $z/D = 4$ and 5 respectively.

Furthermore, it seems interesting to compare the value of the numerically resolved R_{yz} and simulated (subgrid-scale) turbulent stresses for these cross sections . The latter can be assessed by multiplying the characteristic subgrid-scale viscosity by the maximum value of the velocity gradient, estimated from the profiles shown in Fig. 5. According to the data in Fig. 4,*d*, the molecular viscosity can be taken as the characteristic value of subgrid-scale viscosity. As a consequence, the estimated value of $\tau_{SGS}/V_b^2 \cong$ is 0.005, which is only 2 – 3 % of the level of numerically resolved turbulent stresses.

The quantities k and Ryz decrease rapidly with distance from the sections $z/D = 4$ and 5. The profiles of both quantities have local maxima at $y/D \cong 0.6$ for the section $z/D = 2$: on the one hand, the average velocity profile here is characterized by large gradients (Fig. 5) and, on the other hand, the manifestation of hydrodynamic instabilities is fairly pronounced (see Fig. 4,*b*).

Conclusion

We have applied large eddy simulation with the Germano – Lilly dynamic model of subgrid-scale viscosity for numerical study of substantially three-dimensional flow developing at a Reynolds number Re = 1803 in a blood vessel with unilateral stenosis of 70%. The computations performed revealed the following peculiarities of the flow.

The averaged motion in the region behind stenosis is characterized by the presence of two zones with recirculation flow: an extensive one developing directly behind the stenosis, and a small one, located near the opposite wall of vessel.

As a jet with relatively high local velocities is generated in the stenotic region, rather intense secondary flow also develops, taking the form of a pair of vortices, similar to Dean vortices in curved tubes. In turn, the vortex pair evolving in the stenosis induces secondary backflow behind the stenosis, also leading to bifurcation of the jet.

The cross flow is almost completely degenerate at a distance of less than 10 calibers (diameters of the vessel) from the stenosis. A high-gradient mixing layer forms at the boundary between the jet and the backflow zone. The hydrodynamic instabilities inherent to this layer generate turbulence in the flow, with three-dimensional vortical structures of different scales forming, which fill the entire cross-section of vessel in the neighborhood of the attachment point, located at a distance of approximately five calibers from the center of stenosis.

Shear turbulent stresses only have substantial values in the zone with the size of about 4 calibers in the neighborhood of the attachment point. The flow is relaminarized downstream.

We believe that applying the LES method is bound to improve the quality of predicting the characteristics of turbulence developing during blood flow through stenotic regions of the vascular bed, and, as a consequence, provide more reliable data of interest for biomedicine.

This study was financially supported by the Russian Science Foundation, grant No. 19-73-30003.

REFERENCES

1. **Gataulin Ya.A., Zaitsev D.K., Smirnov E.M., et al.,** Weakly swirling flow in a model of blood vessel with stenosis: Numerical and experimental study, St. Petersburg State Polytechnical University Journal. Physics and Mathematics. (4(230)) (2015) 36–47.

2. **Gataulin Ya.A., Zaitsev D.K., Smirnov E.M., Yukhnev A.D.,** Numerical study of spatial-temporal evolution of the secondary flow in the models of a common carotid artery, St. Petersburg State Polytechnical University Journal. Physics and Mathematics. (4(253)) (2016) 48–55.

3. **Gataulin Y.A., Zaitsev D.K., Smirnov E.M.,**

Yukhnev A.D., Structure of unsteady flow in the spatially curved model of the common carotid artery with stenosis: A numerical study, Russian Journal of Biomechanics. 23 (1) (2019) 58–66.

4. **Ghalichi F., Farzan G., Deng X., et al.,** Low Reynolds number turbulence modeling of blood flow in arterial stenosis, Biorheology. 35 (4, 5) (1998) 281–294.

5. **Varghese S.S., Frankel S.H.,** Numerical modeling of pulsatile turbulent flow in stenotic vessels, Journal of Biomechanical Engineering. 125 (4) (2003) 445–460.

6. **Lee T.S., Liao W., Low H.T.,** Numerical study of physiological turbulent flows through series arterial stenosis, International Journal for Numerical Methods in Fluids. 46 (3) (2004) 315–344.

7. **Li M.X, Beech-Brandt J.J., John L.R., et al.,** Numerical analysis of pulsatile blood flow and vessel wall mechanics in different degrees of stenosis, Journal of Biomechanics. 40 (16) (2007) 3715–3724.

8. **Sherwin S.J., Blackburn H.M.,** Three-dimensional instabilities and transition of steady and pulsatile flows in an axisymmetric stenotic flows, Journal of Fluid Mechanics. 533 (25 June) (2005) 297–327.

9. **Blackburn H.M., Sherwin S.J.,** Instability modes and transition of pulsatile stenotic flow: pulse-period dependence, Journal of Fluid Mechanics. 573 (February) (2007) 57–88.

10. **Varghese S.S., Frankel S.H., Fischer P.F.,** Direct numerical simulation of stenotic flows. Part 1. Steady flow, Journal of Fluid Mechanics. 582 (10 July) (2007) 253–280.

11. **Varghese S.S., Frankel S.H., Fischer P.F.,** Direct numerical simulation of stenotic flows. Part 2. Pulsatile flow, Journal of Fluid Mechanics. 582 (10 July) (2007) 281–318.

12. **Mittal R., Simmons S.P., Udaykumar H.S.,** Application of large-eddy simulation to the study of pulsatile flow in a modelled arteria stenosis, Journal of Biomechanical Engineering. 123 (4) (2001) 325–332.

13. **Mittal R., Simmons S.P., Najjar F.,** Numerical study of pulsatile flow in a constricted channel, Journal of Fluid Mechanics. 485 (25 May) (2003) 337–378.

14. **Molla M.M., Paul M.C., Roditi G.,** LES of additive and non-additive pulsatile flows in a model arterial stenosis, Computer Methods in Biomechanics and Biomedical Engineering. 13 (1) (2010) 105–120.

15. **Paul M.C., Molla M.M.,** Investigation of physiological pulsatile flow in a model arterial stenosis using large-eddy and direct numerical simulations // Applied Mathematical Modelling. 36 (9) (2012) 4393–4413.

16. **Germano M., Piomelli U., Moin P., Cabot W.H.,** A dynamic subgridscale eddy viscosity model, Physics of Fluids. 3 (7) (1991) 1760–1765.

17. **Lilly D.K.,** A proposed modification of the Germano subgrid-scale closure method, Physics of Fluids. 4 (3) (1992) 633–635.

18. **Choi W., Park J.H., Byeon H., Lee S.J.,** Flow characteristics around a deformable stenosis under pulsatile flow condition, Physics of Fluids. 30 (1) (2018) 011902.

19. **Jeong J., Hussain F.,** On the identification of a vortex, Journal of Fluid Mechanics. 285 (25 February) (1995) 69–94.

Received 29.12.2020, accepted 10.02.2021.

THE AUTHORS

GATAULIN Yakov A.
Peter the Great St. Petersburg Polytechnic University
29 Politechnicheskaya St., St. Petersburg, 195251, Russian Federation
yakov_gataulin@mail.ru

SMIRNOV Evgeny M.
Peter the Great St. Petersburg Polytechnic University
29 Politechnicheskaya St., St. Petersburg, 195251, Russian Federation
smirnov_em@spbstu.ru

СПИСОК ЛИТЕРАТУРЫ

1. **Гатаулин Я.А., Зайцев Д.К., Смирнов Е.М., Федорова Е.А., Юхнев А.Д.** Расчетно-экспериментальное исследование слабо закрученного течения в модели сосуда со стенозом // Научно-технические ведомости СПбГПУ. Физико-математические науки. 2015. № 4 (230). С. 36–47.

2. **Гатаулин Я.А., Зайцев Д.К., Смирнов Е.М., Юхнев А.Д.** Численное исследование пространственно-временной эволюции вторичного течения в модели общей сонной артерии // Научно-технические ведомости СПбГПУ. Физико-математические науки. 2016. № 4 (253). С. 48–55.

3. **Гатаулин Я.А., Зайцев Д.К., Смирнов Е.М., Юхнев А.Д.** Структура нестационарного течения в пространственно-извитой модели общей сонной артерии со стенозом: численное исследование // Российский журнал биомеханики. 2019. Т. 23. № 1. С. 69–78.

4. **Ghalichi F., Farzan G., Deng X., Champlain A.D., Douville Y., King M., Guidoin R.** Low Reynolds number turbulence modeling of blood flow in arterial stenoses // Biorheology. 1998. Vol. 35. No. 4, 5. Pp. 281–294.

5. **Varghese S.S., Frankel S.H.** Numerical modeling of pulsatile turbulent flow in stenotic vessels // Journal of Biomechanical Engineering. 2003. Vol. 125. No. 4. Pp. 445–460.

6. **Lee T.S., Liao W., Low H.T.** Numerical study of physiological turbulent flows through series arterial stenoses // International Journal for Numerical Methods in Fluids. 2004. Vol. 46. No. 3. Pp. 315–344.

7. **Li M.X, Beech-Brandt J.J., John L.R., Hoskins P.R., Easson W.J.** Numerical analysis of pulsatile blood flow and vessel wall mechanics in different degrees of stenoses // Journal of Biomechanics. 2007. Vol. 40. No. 16. Pp. 3715–3724.

8. **Sherwin S.J., Blackburn H.M.** Three-dimensional instabilities and transition of steady and pulsatile flows in an axisymmetric stenotic flows // Journal of Fluid Mechanics. 2005. Vol. 533. 25 June. Pp. 297–327.

9. **Blackburn H.M., Sherwin S.J.** Instability modes and transition of pulsatile stenotic flow: pulse-period dependence // Journal of Fluid Mechanics. 2007. Vol. 573. February. Pp. 57–88.

10. **Varghese S.S., Frankel S.H., Fischer P.F.** Direct numerical simulation of stenotic flows. Part 1. Steady flow // Journal of Fluid Mechanics. 2007. Vol. 582. 10 July. Pp. 253–280.

11. **Varghese S.S., Frankel S.H., Fischer P.F.** Direct numerical simulation of stenotic flows. Part 2. Pulsatile flow // Journal of Fluid Mechanics. 2007. Vol. 582. 10 July. Pp. 281–318.

12. **Mittal R., Simmons S.P., Udaykumar H.S.** Application of large-eddy simulation to the study of pulsatile flow in a modelled arteria stenosis // Journal of Biomechanical Engineering. 2001. Vol. 123. No. 4. Pp. 325–332.

13. **Mittal R., Simmons S.P., Najjar F.** Numerical study of pulsatile flow in a constricted channel // Journal of Fluid Mechanics. 2003. Vol. 485. 25 May. Pp. 337–378.

14. **Molla M.M., Paul M.C., Roditi G.** LES of additive and non-additive pulsatile flows in a model arterial stenosis // Computer Methods in Biomechanics and Biomedical Engineering. 2010. Vol. 13. No. 1. Pp. 105–120.

15. **Paul M.C., Molla M.M.** Investigation of physiological pulsatile flow in a model arterial stenosis using large-eddy and direct numerical simulations // Applied Mathematical Modelling. 2012. Vol. 36. No. 9. Pp. 4393–4413.

16. **Germano M., Piomelli U., Moin P., Cabot W.H.** A dynamic subgridscale eddy viscosity model // Physics of Fluids. 1991. Vol. 3. No. 7. Pp. 1760–1765.

17. **Lilly D.K.** A proposed modification of the Germano subgrid-scale closure method // Physics of Fluids. 1992. Vol. 4. No. 3. Pp. 633–635.

18. **Choi W., Park J.H., Byeon H., Lee S.J.** Flow characteristics around a deformable stenosis under pulsatile flow condition // Physics of Fluids. 2018. Vol. 30. No. 1. P. 011902.

19. **Jeong J., Hussain F.** On the identification of a vortex // Journal of Fluid Mechanics. 1995. Vol. 285. 25 February. Pp. 69–94.

Статья поступила в редакцию 29.12.2020, принята к публикации 10.02.2021.

СВЕДЕНИЯ ОБ АВТОРАХ

ГАТАУЛИН Яков Александрович – *математик, заместитель директора Института прикладной математики и механики по научно-исследовательской работе студентов Санкт-Петербургского политехнического университета Петра Великого, Санкт-Петербург, Российская Федерация.*

195251, Российская Федерация, г. Санкт-Петербург, Политехническая ул., 29

yakov_gataulin@mail.ru

СМИРНОВ Евгений Михайлович – *доктор физико-математических наук, профессор Высшей школы прикладной математики и вычислительной физики Санкт-Петербургского политехнического университета Петра Великого, Санкт-Петербург, Российская Федерация.*

195251, Российская Федерация, г. Санкт-Петербург, Политехническая ул., 29

smirnov_em@spbstu.ru

© Санкт-Петербургский политехнический университет Петра Великого, 2021